available at www.sciencedirect.com
journal homepage: www.europeanurology.com

European Association of Urology

Surgery in Motion

The Use of Augmented Reality to Guide the Intraoperative Frozen Section During Robot-assisted Radical Prostatectomy

Lorenzo Bianchi [a,b,†,*], *Francesco Chessa* [a,b,†], *Andrea Angiolini* [a,b,c], *Laura Cercenelli* [c,d], *Simone Lodi* [e], *Barbara Bortolani* [c], *Enrico Molinaroli* [a], *Carlo Casablanca* [a], *Matteo Droghetti* [a], *Caterina Gaudiano* [f], *Angelo Mottaran* [a], *Angelo Porreca* [g], *Rita Golfieri* [b,f], *Daniele Romagnoli* [g], *Francesca Giunchi* [h], *Michelangelo Fiorentino* [h], *Pietro Piazza* [a,i,j], *Stefano Puliatti* [i,j,k], *Stefano Diciotti* [e], *Emanuela Marcelli* [c], *Alexandre Mottrie* [i,j], *Riccardo Schiavina* [a,b]

[a] *Division of Urology, IRCCS Azienda Ospedaliero-Universitaria di Bologna, University of Bologna, Bologna, Italy;* [b] *Università degli Studi di Bologna, Bologna, Italy;* [c] *Department of Experimental, Diagnostic and Specialty Medicine (DIMES), Laboratory of Bioengineering, University of Bologna, Bologna, Italy;* [d] *Department of Biomedical and Neuromotor Sciences (DIBINEM), University of Bologna, Bologna, Italy;* [e] *Department of Electrical, Electronic and Information Engineering "Guglielmo Marconi", University of Bologna, Bologna, Italy;* [f] *Department of Radiology, IRCCS Azienda Ospedaliero-Universitaria di Bologna, University of Bologna, Bologna, Italy;* [g] *Department of Urology, Abano Terme Hospital, Padua, Italy;* [h] *Pathology Department, IRCCS Azienda Ospedaliero-Universitaria di Bologna, University of Bologna, Bologna, Italy;* [i] *Department of Urology, OLV Hospital, Aalst, Belgium;* [j] *ORSI Academy, Melle, Belgium;* [k] *Department of Urology, University of Modena and Reggio Emilia, Modena, Italy*

Article info

Article history:
Accepted June 24, 2021

Associate Editor:
Alexandre Mottrie

Keywords:
Augmented reality
Three-dimensional
reconstruction

Please visit www.europeanurology.com and www.urosource.com to view the accompanying video.

Abstract

Background: Multiparametric magnetic resonance imaging (mpMRI) can guide the surgical plan during robot-assisted radical prostatectomy (RARP), and intraoperative frozen section (IFS) can facilitate real-time surgical margin assessment.
Objective: To assess a novel technique of IFS targeted to the index lesion by using augmented reality three-dimensional (AR-3D) models in patients scheduled for nerve-sparing RARP (NS-RARP).
Design, setting, and participants: Between March 2019 and July 2019, 20 consecutive prostate cancer patients underwent NS-RARP with IFS directed to the index lesion with the help of AR-3D models (study group). Control group consists of 20 patients matched with 1:1 propensity score for age, clinical stage, Prostate Imaging Reporting and Data System score v2, International Society of Urological Pathology grade, prostate volume, NS approach, and prostate-specific antigen in which RARP was performed by cognitive assessment of mpMRI.
Surgical procedure: In the study group, an AR-3D model was superimposed to the surgical field to guide the surgical dissection. Tissue sampling for IFS was taken in the area in which the index lesion was projected by AR-3D guidance.
Measurements: Chi-square test, Student *t* test, and Mann-Whitney *U* test were used to compare, respectively, proportions, means, and medians between the two groups.
Results and limitations: Patients in the AR-3D group had comparable preoperative characteristics and those undergoing the NS approach were referred to as the control group (all $p \geq 0.06$). Overall, positive surgical margin (PSM) rates were comparable between the two groups; PSMs at the level of the index lesion were significantly lower in

† Both these authors contributed equally to this work.
* Corresponding author. Division of Urology, IRCCS Azienda Ospedaliero-Universitaria di Bologna, University of Bologna, Bologna, Italy. Tel. +39 051 6362747; Fax: +39 0516362535.
E-mail address: lorenzo.bianchi3@gmail.com (L. Bianchi).

https://doi.org/10.1016/j.eururo.2021.06.020

Keywords:
Intraoperative frozen section
Prostate cancer
Robot-assisted radical prostatectomy

patients referred to AR-3D guided IFS to the index lesion (5%) than those in the control group (20%; $p = 0.01$).
Conclusions: The novel technique of AR-3D guidance for IFS analysis may allow for reducing PSMs at the level of the index lesion.
Patient summary: Augmented reality three-dimensional guidance for intraoperative frozen section analysis during robot-assisted radical prostatectomy facilitates the real-time assessment of surgical margins and may reduce positive surgical margins at the index lesion.

1. Introduction

Positive surgical margins (PSMs) during radical prostatectomy (RP) are strong predictors of biochemical recurrence [1–3]. Thus, different surgical techniques were introduced to reduce PSMs [1], and several methods have been proposed for "real-time" evaluation of surgical margins [4]. Cognitive guidance of multiparametric magnetic resonance imaging (mpMRI) during robot-assisted RP (RARP) may improve the preservation of neurovascular bundles (NVBs) and avoid PSMs [5–7]. An intraoperative frozen section (IFS) analysis is the most commonly used technique for real-time assessment of surgical margins during RARP [4], despite some authors reporting low sensitivity [8,9]. Moreover, the ways to collect samples for IFS include different techniques [10]. A systematic IFS analysis was originally proposed to monitor the safety of nerve sparing (NS), using a whole neurovascular structure–adjacent frozen section examination (NeuroSAFE) [11]: significant increase of NS and reduction in PSMs were reported, without compromising oncological safety [11–13]. Alternatively, IFS can be directed to the index lesion detected by mpMRI since larger-volume index lesions are responsible for the vast majority of PSMs [5]. Indeed, Petralia et al [14] reported that mpMRI-directed IFS was able to reduce the risk of PSMs. However, this approach is limited by a cognitive evaluation during surgery. In the era of patient-tailored surgery, the augmented reality (AR) technology by overlapping anatomical three-dimensional (3D) models in the robotic view could facilitate the intraoperative navigation by identifying the index lesion and guiding IFS samples. In this study, we aimed to assess a novel technique of AR-3D guided IFS for real-time assessment of surgical margins during NS RARP and to evaluate the impact of this novel approach on PSMs.

2. Patients and methods

We prospectively enrolled patients with a diagnosis of prostate cancer (PCa) on the basis of positive mpMRI-targeted fusion biopsy at the index lesion [15] and preoperative preserved erectile function (International Index of Erectile Function-5 [IIEF-5] questionnaire score >21 [16]) scheduled for NS RARP at a single tertiary center. The study was conducted in accordance with the Good Clinical Practice after Institutional Ethics Committee (IRB approval 4325/2017), and informed consent was obtained from each patient. Exclusion criteria were absolute contraindications for robotic surgery, no index lesion at mpMRI, index lesion at mpMRI located in the transitional zone or far away from the prostatic capsule and the apex, and mpMRI not available.

2.1. Study group

Overall, 20 consecutive PCa patients with an index lesion detected at preoperative mpMRI underwent RARP between March 2019 and July 2019. Prior to the intervention, patients enrolled were addressed to undergo 3D virtual model reconstruction based on preoperative mpMRI images. Finally, the surgeon performed RARP with the help of the 3D model projected in AR inside the robotic console (AR-3D guided RARP) with the implementation of a real-time IFS analysis directed to the index lesion projected by the AR-3D guidance.

2.2. Control group

Overall, 167 PCa patients with an index lesion at preoperative mpMRI and with complete clinical, intraoperative, and pathological data underwent standard mpMRI guided NS RARP from January 2019 to July 2019 without the aid of the AR-3D technology or IFS analysis.

To reduce the inherent differences between patients undergoing mpMRI guided RARP and those referred to AR-3D guided RARP with an IFS analysis, we used a 1:1 propensity score–matched analysis adjusted for age, clinical stage based on mpMRI, Prostate Imaging Reporting and Data System (PI-RADS) v2 score [17], clinical International Society of Urological Pathology (ISUP) grade, prostate volume, NS approach, and preoperative prostate-specific antigen. The matched population ($n = 40$) included 20 patients in the study group and 20 in the control group.

2.3. Multiparametric MRI

All the mpMRI examinations in both groups were performed with a 1.5-T whole-body scanner (Signa HDxt; GE Healthcare, Milwaukee, WI, USA) and a standard eight-channel pelvic phased-array surface coil combined with a disposable endorectal coil (MedRad, Indianola, PA, USA) as previously described [7,18]. All lesions were scored using the PI-RADS-v2 score [17] and centrally reviewed by one experienced radiologist. The index lesion is the lesion with the highest PI-RADS-v2 assessment category [17].

2.4. Three-dimensional model

All 3D virtual models were based on preoperative mpMRI, as previously described [19–21]. Semiautomatic tools (multislice interpolation and threshold segmentation) of D2P software (3D Systems Inc., Rock Hill, SC, USA) were adopted to segment the healthy prostatic gland, index lesion, urinary sphincter, and NVBs [20]. D2P was also used to obtain 3D virtual models (Fig. 1A and 1B).

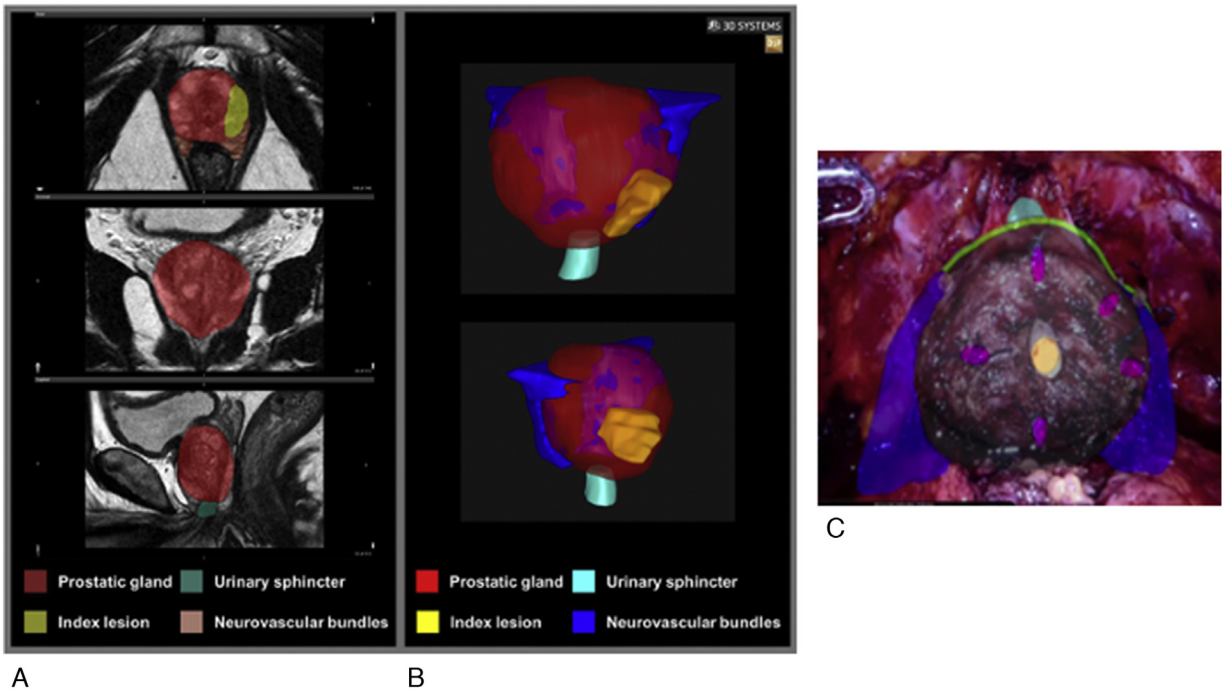

Fig. 1 – (A) The 3D virtual anatomical model is obtained starting from patient mpMRI, by the segmentation of the anatomical regions of interest (prostatic gland, index lesion, urinary sphincter, and neurovascular bundles) to (B) the final 3D model (C) that is overlapped in the robotic view through the AR technology. AR = augmented reality; 3D = three dimensional; mpMRI = multiparametric magnetic resonance imaging.

2.5. Augmented reality

The surgical video stream has been acquired from the DaVinci video cart via a frame grabber (USB3HD; Startech, London, Ontario, Canada) and sent to an AR-dedicated PC (equipped with an Intel i7 CPU, 8 GB RAM and NVIDIA GeForce 840M video card). A 3D view of the virtual model obtained using Meshmixer software (Autodesk Inc., San Rafael, CA, USA) was superimposed on the aforementioned operatory field with vMIX (StudioCoast Pty Ltd, Robina, Queensland, Australia), as previously described [20]. The DaVinci TilePro has been activated in the console (Fig. 1C), and real-time manual alignment has been carried out by a biomedical engineer using a (3D) mouse with six degrees of freedom (SpaceMouse; 3D Connexion, Munich, Germany).

2.6. Surgical technique

All patients underwent RARP using the four-arm DaVinci Xi Surgical System (Intuitive Surgical, Sunnyvale, CA, USA), as described previously [22–25], by a single experienced robotic surgeon (R.S.). The NS approaches were classified on patient-based level as bilateral NS, unilateral NS, or non-NS. Indeed, the extent of NVB preservation was recorded on side-based level as grades 1, 2, and 3–4 [26].

2.7. AR-3D guided RARP with IFS

The AR-3D superimposed model was used to identify the site of the index lesion during RARP (Fig. 2A and 2B) and to drive the surgical dissection of crucial steps (namely, apex, bladder neck, and NS), through TilePro visualization [20,21]. Therefore, a sample from the periprostatic tissue was taken in the periprostatic area in which the index lesion is projected by AR-3D guidance (Fig. 2C and 2D) and sent for IFS (first IFS). Different behavior was adopted according to tumor location: in case of posterolateral location of the index lesion, if presence of PCa cells is detected in the first IFS, complete resection of the ipsilateral NVB was performed and the sample was sent for second IFS. In case of apical or bladder neck location of the index lesion, after a first positive IFS, partial resection of periprostatic tissue was performed and it was sent for a second IFS analysis at apical or basal aspect, respectively.

2.8. Standard mpMRI guided RARP

During standard RARP, intraoperative dissection of NVBs, the bladder neck, and the apex was guided by clinical data and cognitive evaluation of mpMRI information without the implementation of an IFS analysis, as described previously [7].

2.9. Histopathological examination

All the pathological examinations including the first and second IFS samples were evaluated by a single dedicated uropathologist. The whole mount histological examinations from the RARP specimens were performed following a prostate map, as described previously [20]. Surgical margins (overall and at the level of the index lesion) were considered positive if tumor cells are in contact with the ink on the specimen surface. The tissues for the IFS analysis were prepared for staining with hematoxylin and eosin for microscopic examination: presence of PCa cells in IFS samples was considered positive (Fig. 3A and 3B).

2.10. Statistical analyses

Chi-square test, Student *t* test, and Mann-Whitney test were used to compare, respectively, proportions, means, and medians between the study and control groups. The McNemar-Bowker test was used to evaluate the concordance between the index lesion detected by mpMRI-

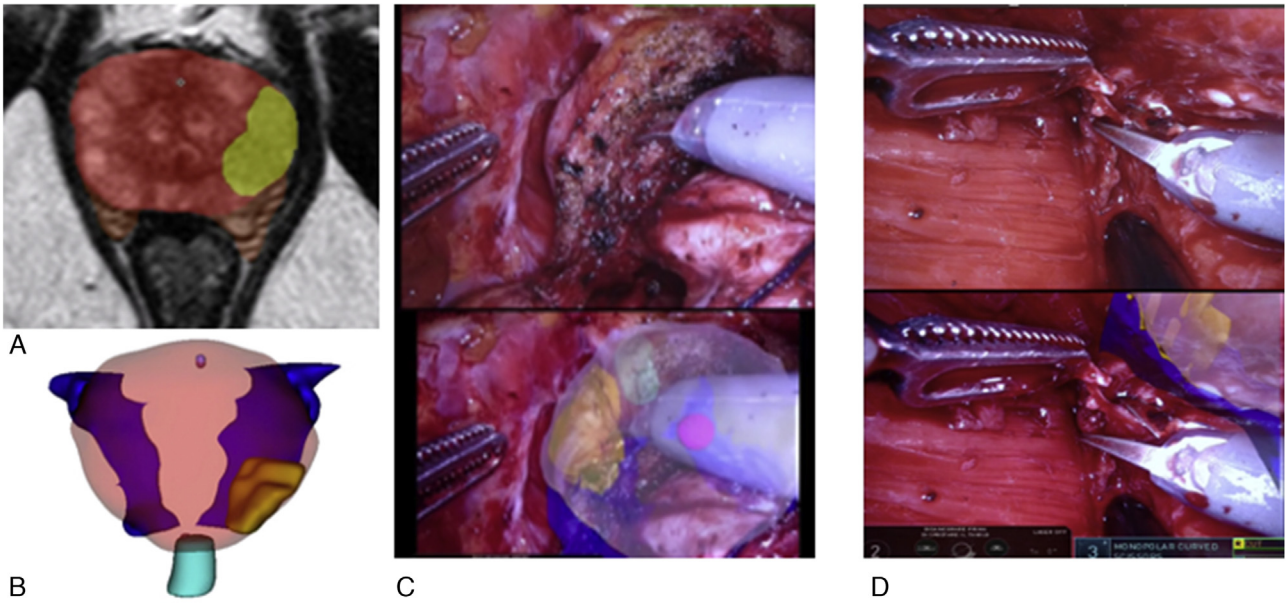

Fig. 2 – Example of AR-3D guided surgical dissection for real-time assessment of the index lesion during the nerve-sparing RARP through TilePro visualization and AR-3D guided IFS analysis. (A) A 17-mm left posterolateral apical index lesion PI-RADS v.2 score 5 (yellow area) is detected by mpMRI (Gleason score 3 + 4 in six cores at fusion-targeted biopsy). (B) The 3D model is employed with reconstruction of the index lesion (yellow), prostate glands (pink), urethra (light blue), and neurovascular bundles (blue). (C) AR-3D guided RARP with IFS analysis targeted to the projected index lesion was performed. (D) A first sample of the posterolateral periprostatic tissue is taken for IFS analysis at the level of the index lesion guided by AR. The first frozen section was found to be negative for tumoral cells; thus, the surgeon performed a grade 2 nerve sparing on the left side, modulating the dissection in real time, avoiding a plane of dissection too close to the level of the index lesion. AR = augmented reality; 3D = three dimensional; IFS = intraoperative frozen section; mpMRI = multiparametric magnetic resonance imaging; PI-RADS = Prostate Imaging Reporting and Data System; RARP = robot-assisted radical prostatectomy.

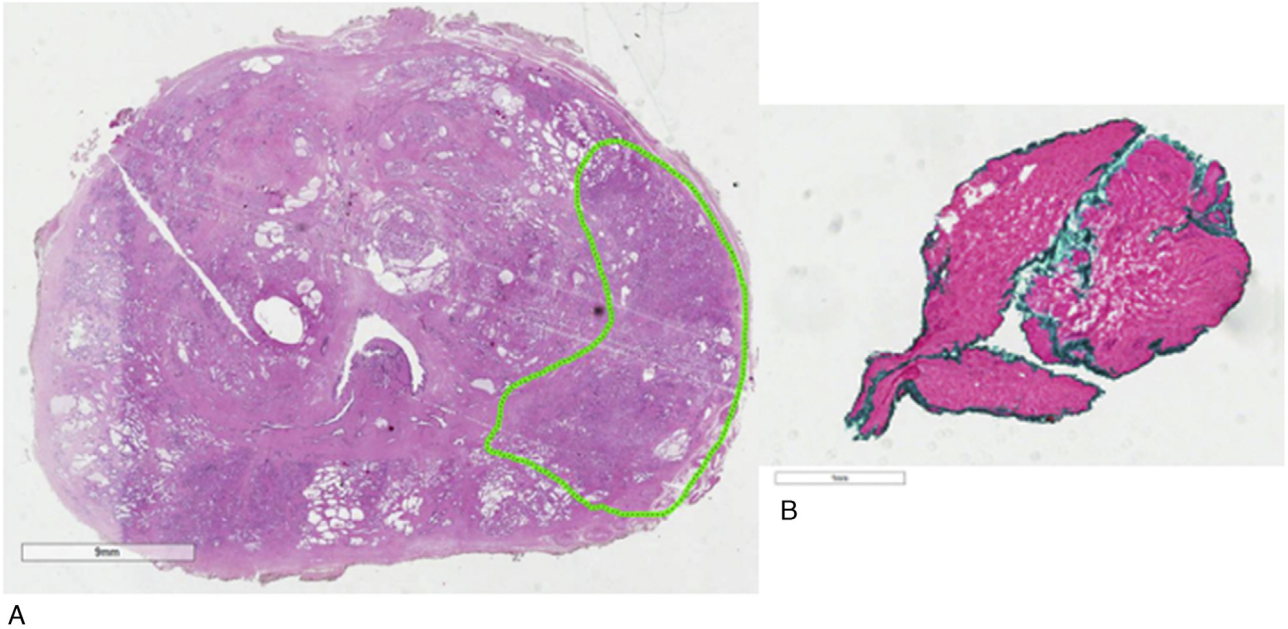

Fig. 3 – (A) The whole mount prostate specimen revealed a predominant left apical tumor (Gleason score 4 + 3 pT3a) with negative surgical margins. (B) The index lesion is covered by a thin layer of periprostatic tissue and the final pathological reports of IFS analysis targeted to the index lesion confirmed the absence of prostate cancer cells. IFS = intraoperative frozen section.

derived 3D model in the study group or mpMRI in the control group, and the index lesion identified at final pathology. All statistical tests were performed using the R statistical package (R Foundation for Statistical Computing, Vienna, Austria) with a two-sided significance level set at $p < 0.05$.

3. Results

After matching 1:1, there were no significant differences between the two groups concerning the covariate used for

the propensity score match (all $p \geq 0.06$; Tables 1 and 2). Preoperative mpMRI reported organ-confined index lesion, suspected extracapsular extension, and seminal vesicle invasion in 17 (80%), three (20%), and zero (0%) patients referred to the AR-3D guided IFS approach and in 15 (75%), four (20%), and one (5%) patients referred to the mpMRI guided approach, respectively ($p = 0.2$; Supplementary Tables 1 and 2). The mean console time and estimated blood loss were comparable between the AR-3D group (216 min and 200.2 ml, respectively) and the control group (208 min and 182.5 ml, respectively; all $p \geq 0.06$; Table 2). Patients in the study group received similar proportion of unilateral and bilateral NS on patient-based and grade 1, 2, and 3–4 NS on side-based analysis, compared with those in the control group (all $p \geq 0.3$). In four patients, the AR-3D guided IFS analysis (first sample) revealed the presence of residual PCa cells in the periprostatic tissue in contact with the index lesion (two apical and two posterolateral location). All these patients underwent a secondary resection (second sample) of periprostatic tissue, the results of which were negative for the presence of PCa in all cases, contributing to conversion into negative surgical margins in three patients at final pathology: only one out of four patients revealed PSMs outside the index lesion. In 16 patients, the AR-3D guided IFS analysis (first sample) was negative for PCa and resulted in negative surgical margins in 14 patients at final pathology: two men revealed PSMs, including one PSM at the level of the index lesion (Fig. 4). Overall, PSM rates were comparable in the study and control groups (15% vs 20%, $p = 0.2$; Table 3). Similarly, no differences were found between the two groups concerning PSM rates after stratifying according to pathological stage and site of PSMs. However, PSMs at the level of the index lesion were significantly lower in patients referred to AR-3D guided IFS directed to the index lesion (5%) than in the control group (20%, $p = 0.02$; Table 3).

Table 1 – Patient characteristics and descriptive statistics in the matched population after 1:1 propensity score matching ($n = 40$)

	Overall ($n = 40$)	AR-3D guided IFS RARP ($n = 20$)	mpMRI guided RARP ($n = 20$)	p value
Age				
Median	62	62	62	0.8
IQR	55–70	56–71	54–69	
PSA (ng/ml)				
Median	9	6.6	10	0.3
IQR	7–9	5–8	8.3–11	
ASA score, *n* (%)				
1–2	35 (87.5)	18 (90)	17 (85)	0.3
3	5 (12.5)	2 (10)	3 (15)	
IIEF-5				
Median	23	23	22	0.07
IQR	21–24	22–24	21–24	
mpMRI results, *n* (%)				
Organ confined	32 (80)	17 (85)	15 (75)	0.2
ECE	7 (17.5)	3 (15)	4 (20)	
SVI	1 (2.5)	0 (0)	1 (5)	
Prostate volume at mpMRI (ml)				
Median	50	50	48	0.08
IQR	30–60	35–60	30–58	
PI-RADS-v.2 score, *n* (%)				
3	14 (35)	7 (35)	7 (35)	0.3
4	16 (40)	7 (35)	9 (45)	
5	10 (25)	6 (30)	4 (20)	
mpMRI index lesion's size (mm), mean ± SD	15.3 ± 6.2	16.4 ± 7.1	14 ± 5.8	0.5
Site of the index lesion at mpMRI, *n* (%)				
Apex—anterior	15 (37.5)	8 (40)	7 (35)	0.5
Posterolateral	15 (37.5)	7 (35)	8 (40)	
Base—bladder neck	10 (25)	5 (25)	5 (25)	
Clinical ISUP grade, *n* (%)				
1	4 (10)	2 (10)	2 (10)	0.3
2	13 (32.5)	9 (45)	4 (20)	
3	11 (27.5)	5 (25)	6 (30)	
4	10 (25)	4 (20)	6 (30)	
5	2 (5)	0 (0)	2 (10)	
Bioptic cores taken				
Median	12	12	12	0.7
IQR	12–14	12–14	12–14	
Positive bioptic cores				
Median	4	4	6	0.5
IQR	3–7	1–6	3–8	

AR-3D = augmented reality three dimensional; ASA = American Society of Anesthesiologists; ECE = extracapsular extension; IFS = intraoperative frozen section; IIEF-5 = International Index of Erectile Function-5; IQR = interquartile range; ISUP = International Society of Urological Pathology; mpMRI = multiparametric magnetic resonance imaging-guided; PI-RADS = Prostate Imaging Reporting and Data System; PSA = prostate-specific antigen; RARP = robot-assisted radical prostatectomy; SD = standard deviation; SVI = seminal vesicle invasion.
Patients are stratified according to the surgical approach (namely, AR-3D guided IFS RARP and mpMRI guided RARP).

Table 2 – Intraoperative, pathological, and postoperative outcomes in the matched population after 1:1 propensity score matching (*n* = 40)

	Overall (*n* = 40)	AR-3D guided IFS RARP (*n* = 20)	mpMRI guided RARP (*n* = 20)	*p* value
Overall surgical time, mean ± SD	212.5 ± 54.4	216.2 ± 57.9	208.8 ± 50.8	0.5
Nerve-sparing approach, *n* (%)				
Not performed	8 (20)	2 (10)	6 (30)	0.5
Unilateral	11 (27.5)	5 (25)	6 (30)	
Bilateral	21 (52.5)	13 (65)	8 (40)	
Side-based nerve-sparing grade, *n* (%)				
1	28 (35)	17 (42.5)	11 (27.5)	0.3
2	20 (25)	9 (22.5)	11 (27.5)	
3–4	32 (40)	14 (35)	18 (45)	
Estimated blood loss (ml), mean ± SD	191.4 ± 52.9	200.2 ± 56.3	182.5 ± 49.4	0.06
Pathological stage, *n* (%)				
pT2	17 (42.5)	10 (50)	7 (35)	0.4
pT3a	20 (50)	8 (40)	12 (60)	
pT3b	3 (7.5)	2 (10)	1 (5)	
Pathological ISUP grade, *n* (%)				
1	2 (2)	0 (0)	0 (0)	
2	46 (45.1)	10 (50)	7 (35)	0.5
3	32 (31.4)	5 (25)	7 (35)	
4	14 (13.7)	3 (15)	5 (25)	
5	8 (7.8)	2 (10)	1 (5)	
Postoperative complications, *n* (%)				
No	37 (92.5)	18 (90)	19 (95)	0.07
Yes	3 (7.5)	2 (10)	1 (5)	
Postoperative complication type, *n* (%)				
Lymphocele	2 (5)	1 (5)	1 (5)	0.8
Bleeding requiring blood transfusion	1 (2.5)	1 (5)	0 (0)	
Clavien grade complications, *n* (%)				
1–2	2 (5)	1 (5)	1 (5)	0.8
≥3	1 (2.5)	1 (5)	0 (0)	
Hospital stay (d)				
Median	3	3	3	0.4
IQR	3–4	3–4	3–3	
Catheterization time (d)				
Median	9	8	10	0.06
IQR	7–10	7–10	8–13	
Continence recovery, *n* (%)				
At catheter removal	21 (52.5)	11 (55)	10 (50)	0.2
1 mo	31 (77.5)	15 (75)	16 (80)	
3 mo	35 (87.5)	17 (85)	18 (90)	
6 mo	36 (90)	18 (90)	18 (90)	
12 mo	38 (95)	19 (95)	19 (95)	
Erectile function recovery [a], *n* (%)				
1 mo	7 (21.8)	4 (22.2)	3 (21.4)	0.06
3 mo	14 (43.8)	9 (50)	5 (35.7)	
6 mo	20 (62.5)	12 (66.6)	8 (57.1)	
12 mo	22 (68.8)	13 (72.2)	9 (64.2)	

AR-3D = augmented reality three dimensional; IFS = intraoperative frozen section; IQR = interquartile range; ISUP = International Society of Urological Pathology; mpMRI = multiparametric magnetic resonance imaging; RARP = robot-assisted radical prostatectomy; SD = standard deviation.
Patients are stratified according to the surgical approach (namely, AR-3D guided IFS RARP and mpMRI guided RARP).
[a] Considering patients referred to the nerve-sparing approach.

4. Discussion

Different surgical techniques were introduced to reduce PSMs [1] and several methods have been proposed for "real-time" evaluation of surgical margins [4].

A systematic IFS analysis of the posterolateral prostatic surface (NeuroSAFE) showed a significantly higher rate of NS approach and lower rates of PSMs with conversion to a definitive negative surgical margin in 86% of cases, suggesting that the benefit of increased NS was not achieved at the expense of higher rates of PSMs with both the open [11] and the robotic approach [13]. Recently, the diffusion of imaging-guided surgery has led to a more selective approach for IFS, despite there being no consensus regarding the appropriate sites, methods, or clinical indications for an IFS analysis [27]. Indeed, the accuracy of mpMRI to identify the dominant index PCa has been proposed as a promising tool for mpMRI guided IFS. Petralia et al [14] reported an 11.3% reduction in PSMs when the site submitted for IFS was selected according to the preoperative mpMRI report. Of note, the added value of mpMRI allows directing an IFS analysis to the areas at the highest risk of PSMs.

However, it is not a "real-time" method to evaluate the surgical anatomy, and the main concern regards the lack of precision to localize the index lesion and the contact with

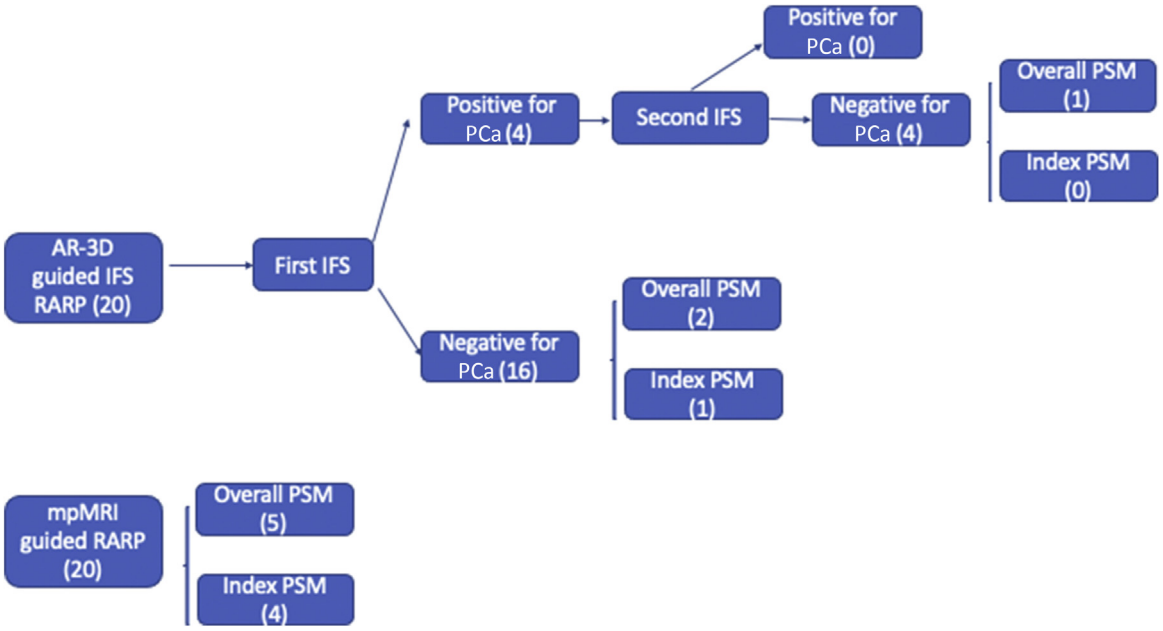

Fig. 4 – Diagram depicts the IFS analysis results and final pathological examinations in patients who underwent AR-3D guided RARP with real-time IFS directed to the index lesion. Findings of the final pathological examinations in matched patients who underwent mpMRI guided RARP (control group) are shown. AR = augmented reality; 3D = three dimensional; IFS = intraoperative frozen section; mpMRI = multiparametric magnetic resonance imaging; PCa = prostate cancer; PSM = positive surgical margin; RARP = robot-assisted radical prostatectomy.

Table 3 – Characteristics of surgical margins in the matched population after 1:1 propensity score matching (*n* = 40)

	Overall (*n* = 40)	AR-3D IFS guided RARP (*n* = 20)	mpMRI guided RARP (*n* = 20)	*p* value
Overall PSM rate, *n* (%)	7 (17.5)	3 (15)	4 (20)	0.2
Overall PSM rates according to pT, *n* (%)				
pT2	1 (5.9)	0 (0)	1 (14.3)	0.08
pT3a	5 (25)	2 (25)	3 (25)	0.8
pT3b	1 (33.3)	1 (50)	0 (0)	0.7
PSM site, *n* (%)				
Apical anterior	3 (42.9)	1 (33.3)	1 (25)	
Posterolateral	3 (42.9)	2 (66.7)	2 (50)	0.1
Bladder neck	1 (14.2)	0 (0)	1 (25)	
PSM at index lesion, *n* (%)	5 (12.5)	1 (5)	4 (20)	0.02
PSM length (mm) [a]				
Median	9	5	9	0.1
IQR	3–17	2–15	7–17	
Gleason score on margin, n (%) [a]				
3	3 (42.9)	1 (33.3)	2 (50)	0.8
4	4 (57.1)	2 (66.7)	2 (50)	

AR-3D = augmented reality three dimensional; IFS = intraoperative frozen section; IQR = interquartile range; mpMRI = multiparametric magnetic resonance imaging; PSM = positive surgical margin; RARP = robot-assisted radical prostatectomy.
Patients are stratified according to the surgical approach (namely, AR-3D guided IFS RARP and mpMRI guided RARP).
[a] Within patients with PSMs.

the periprostatic tissue in real time manner. To note, high-fidelity 3D models represent one of the most appealing methods for better understanding of "in vivo" surgical anatomy and for intraoperative "real-time" navigation during RARP [20,28,29] and robotic renal surgery [21]. Porpiglia and coworkers [28,29] have reported their preliminary experience with the use of AR technology of 3D models, overcoming the cognitive reconstruction and improving surgical outcomes.

The approach proposed in our work is a novel strategy for the application of AR-3D technology to guide surgical dissection during RARP. The current way to use AR-3D guidance is focused to modulate the NS approach tailored to the index lesion, by resecting more tissue nearby the lesion and preserving more tissue outside the lesion [29]. The potential to identify in real time the location of the index lesion during RARP could be used to target the IFS analysis of periprostatic tissue in the area nearby the index lesion overlapped in the robotic view through AR-3D guidance.

Several findings are noteworthy. First, the proposed IFS analysis targeted to the index lesion with AR-3D model's implementation allows modulation of the dissection

directed to the index lesion and improvement of surgical navigation in a personalized manner. Second, the proposed AR-3D guided IFS analysis allows a selective analysis of the periprostatic tissue regardless of the location of the index lesion. Thus, since the larger volume index lesions are responsible for almost all PSMs [5], AR-3D guidance for IFS could have contributed to a significant reduction of PSMs at the index lesion identified by the 3D model compared with that in the control group (5% vs 20%), despite similar overall PSMs and a comparable NS approach. This could be explained with the predominant role of mpMRI and cognitive information to guide NS surgery even without the implementation of an AR-3D model and IFS. Third, our AR-3D guided IFS approach does not significantly prolong the overall surgical time by using the waiting time for an IFS analysis to perform hemostasis, completion of the anastomosis, and lymph node dissection. Finally, 7.5% of postoperative complications were reported, and only one patient (2.5%) experienced grade 3 complications.

Despite several strengths, our study is not devoid of limitations. First, our study could be biased from not modifiable confounding factors due to its retrospective nature. Moreover, the lack of sample size calculation may have reduced the reliability of our findings. However, the adoption of propensity score match aims to reduce the inherent differences between the two groups. Second, the first IFS analysis was targeted to a limited sample of periprostatic tissue in contact with the index lesion, limiting the accuracy of the proposed IFS analysis. Indeed, the major concern of an IFS analysis consists in false negative results, since a wide range in sensitivity and specificity has been reported [4]. Third, we cannot distinguish between the contributions of the AR-3D guided approach and IFS analysis to reduce the PSM rate at the index lesion. However, the overall PSMs were comparable between the two groups, so the real effect of this procedure on oncological outcomes cannot be assess till now. Moreover, most results including the rate of NS procedure could depend on the bias in methodology since the effect of investigatory intervention was not compared with that of the standard procedure in the same group. Fourth, no further IFS was performed in areas outside the index lesion in the study group. Of note, the results of the IFS analysis of periprostatic tissue are strongly related to the level of dissection, since IFS in case of more radical resection of NVBs nearby the index lesion had a higher chance of resulting in negative IFS. Fifth, the presence of PSMs outside the index lesion detected by the AR-3D model and sampled with IFS analyses in two patients (one with pT2a and one with pT3b) indicates a failure of the modality to identify all significant tumor foci by the mpMRI-derived 3D model, in case of bilateral tumors or microscopic involvement of prostatic capsule. Finally, the major limitations of AR-assisted surgery consist of possible registration inaccuracy, translating into a poor navigation precision and the need for manual external adjustments. Automatic registration based on artificial intelligence technology could be a further implementation to reduce manual errors due to manual overlapping of the 3D model inside the DaVinci console for surgical navigation.

5. Conclusions

The proposed technique of AR-3D RARP allows identifying the index lesion in real time and guiding the IFS analysis aimed to reduce PSMs at the level of the index lesion regardless of the location within the prostate. The AR-3D guided approach with IFS targeted to the 3D index lesion could be the evolution of the NeuroSAFE technique.

***Author contributions*:** Lorenzo Bianchi had full access to all the data in the study and takes responsibility for the integrity of the data and the accuracy of the data analysis.

Study concept and design: Bianchi, Chessa, Angiolini, Cercenelli.
Acquisition of data: Lodi, Bortolani, Piazza, Molinaroli, Angiolini.
Analysis and interpretation of data: Casablanca, Gaudiano, Mottaran, Droghetti.
Drafting of the manuscript: Bianchi, Chessa, Cercenelli, Bortolani.
Critical revision of the manuscript for important intellectual content: Porreca, Golfieri, Romagnoli, Giunchi.
Statistical analysis: Bianchi, Chessa, Cercenelli, Droghetti, Casablanca, Gaudiano, Fiorentino, Diciotti.
Obtaining funding: Schiavina, Puliatti, Mottrie.
Administrative, technical, or material support: Diciotti, Marcelli, Lodi, Bortolani, Cercenelli.
Supervision: Marcelli, Diciotti, Mottrie, Schiavina.
Other: None.

***Financial disclosures*:** Lorenzo Bianchi certifies that all conflicts of interest, including specific financial interests and relationships and affiliations relevant to the subject matter or materials discussed in the manuscript (eg, employment/affiliation, grants or funding, consultancies, honoraria, stock ownership or options, expert testimony, royalties, or patents filed, received, or pending), are the following: None.

***Funding/Support and role of the sponsor*:** The project was supported by a Technology Research Grant by Intuitive Surgical for the development of AR technology in robotic surgery.

Appendix A. Supplementary data

The Surgery in Motion video accompanying this article can be found in the online version at doi:https://doi.org/10.1016/j.eururo.2021.06.020 and via www.europeanurology.com.

References

[1] Bianchi L, Turri FM, Larcher A, et al. A novel approach for apical dissection during robot-assisted radical prostatectomy: the “collar” technique. Eur Urol Focus 2018;4:677–85.
[2] Dev HS, Wiklund P, Patel V, et al. Surgical margin length and location affect recurrence rates after robotic prostatectomy. Urol Oncol 2015;33, 109.e7–13.

[3] Yossepowitch O, Bjartell A, Eastham JA, et al. Positive surgical margins in radical prostatectomy: outlining the problem and its long-term consequences. Eur Urol 2009;55:87–99.
[4] Eissa A, Zoeir A, Sighinolfi MC, et al. "Real-time" assessment of surgical margins during radical prostatectomy: state-of-the-art. Clin Genitourin Cancer 2020;18:95–104.
[5] McClure TD, Margolis DJA, Reiter RE, et al. Use of MR imaging to determine preservation of the neurovascular bundles at robotic-assisted laparoscopic prostatectomy. Radiology 2012;262:874–83.
[6] Park BH, Jeon HG, Jeong BC, et al. Influence of magnetic resonance imaging in the decision to preserve or resect neurovascular bundles at robotic assisted laparoscopic radical prostatectomy. J Urol 2014;192:82–8.
[7] Schiavina R, Bianchi L, Borghesi M, et al. MRI displays the prostatic cancer anatomy and improves the bundles management before robot-assisted radical prostatectomy. J Endourol 2018;32:315–21.
[8] Preston MA, Blute ML. Positive surgical margins after radical prostatectomy: does it matter? Eur Urol 2014;65:314–5.
[9] Tsuboi T, Ohori M, Kuroiwa K, et al. Is intraoperative frozen section analysis an efficient way to reduce positive surgical margins? Urology 2005;66:1287–91.
[10] Sighinolfi MC, Eissa A, Spandri V, et al. Positive surgical margin during radical prostatectomy: overview of sampling methods for frozen sections and techniques for the secondary resection of the neurovascular bundles. BJU Int 2020;125:656–66.
[11] Schlomm T, Tennstedt P, Huxhold C, et al. Neurovascular structure-adjacent frozen-section examination (NeuroSAFE) increases nerve-sparing frequency and reduces positive surgical margins in open and robot-assisted laparoscopic radical prostatectomy: experience after 11,069 consecutive patients. Eur Urol 2012;62:333–40.
[12] Preisser F, Theissen L, Wild P, et al. Implementation of intraoperative frozen section during radical prostatectomy: short-term results from a German tertiary-care center. Eur Urol Focus 2021;7(March):95–101.
[13] Beyer B, Schlomm T, Tennstedt P, et al. A feasible and time-efficient adaptation of NeuroSAFE for da Vinci robot-assisted radical prostatectomy. Eur Urol 2014;66:138–44.
[14] Petralia G, Musi G, Padhani AR, et al. Robot-assisted radical prostatectomy: Multiparametric MR imaging-directed intraoperative frozen-section analysis to reduce the rate of positive surgical margins. Radiology 2015;274:434–44.
[15] Ahmed HU. The index lesion and the origin of prostate cancer. N Engl J Med 2009;361:1704–6.
[16] Cappelleri JC, Rosen RC, Smith MD, Mishra A, Osterloh IH. Diagnostic evaluation of the erectile function domain of the International Index of Erectile Function. Urology 1999;54:346–51.
[17] Testa C, Schiavina R, Lodi R, et al. Accuracy of MRI/MRSI-based transrectal ultrasound biopsy in peripheral and transition zones of the prostate gland in patients with prior negative biopsy. NMR Biomed 2010;23:1017–26.
[18] Weinreb JC, Barentsz JO, Choyke PL, et al. PI-RADS Prostate Imaging - Reporting and Data System: 2015, version 2. Eur Urol 2016;69:16–40.
[19] Bianchi L, Barbaresi U, Cercenelli L, et al. The impact of 3D digital reconstruction on the surgical planning of partial nephrectomy: a case-control study. Still time for a novel surgical trend? Clin Genitourin Cancer 2020;18:e669–78.
[20] Schiavina R, Bianchi L, Lodi S, et al. Real-time augmented reality three-dimensional guided robotic radical prostatectomy: preliminary experience and evaluation of the impact on surgical planning. Eur Urol Focus. In press. https://doi.org/10.1016/j.euf.2020.08.004.
[21] Schiavina R, Bianchi L, Chessa F, et al. Augmented reality to guide selective clamping and tumor dissection during robot-assisted partial nephrectomy: a preliminary experience. Clin Genitourin Cancer. In press. https://doi.org/10.1016/j.clgc.2020.09.005.
[22] Porreca A, D'agostino D, Dandrea M, et al. Bidirectional barbed suture for posterior musculofascial reconstruction and knotless vesicourethral anastomosis during robot-assisted radical prostatectomy. Minerva Urol Nefrol 2018;70:319–25.
[23] Porreca A, Salvaggio A, Dandrea M, et al. Robotic-assisted radical prostatectomy with the use of barbed sutures. Surg Technol Int 2017;30:39–43.
[24] Schiavina R, Bertaccini A, Franceschelli A, et al. The impact of the extent of lymph-node dissection on biochemical relapse after radical prostatectomy in node-negative patients. Anticancer Res 2010;30:2297–302.
[25] Farolfi A, Ceci F, Castellucci P, et al. (68)Ga-PSMA-11 PET/CT in prostate cancer patients with biochemical recurrence after radical prostatectomy and PSA <0.5 ng/ml. Efficacy and impact on treatment strategy. Eur J Nucl Med Mol Imaging 2019;46:11–9.
[26] Tewari AK, Ali A, Metgud S, et al. Functional outcomes following robotic prostatectomy using athermal, traction free risk-stratified grades of nerve sparing. World J Urol 2013;31:471–80.
[27] Kakiuchi Y, Choy B, Gordetsky J, et al. Role of frozen section analysis of surgical margins during robot-assisted laparoscopic radical prostatectomy: a 2608-case experience. Hum Pathol 2013;44:1556–62.
[28] Porpiglia F, Checcucci E, Amparore D, et al. Augmented-reality robot-assisted radical prostatectomy using hyper-accuracy three-dimensional reconstruction (HA3D) technology: a radiological and pathological study. BJU Int 2019;123:834–45.
[29] Porpiglia F, Bertolo R, Amparore D, et al. Augmented reality during robot-assisted radical prostatectomy: expert robotic surgeons' on-the-spot insights after live surgery. Minerva Urol Nefrol 2018;70:226–9.